Influence of random point defects introduced by proton irradiation on critical current density and vortex dynamics of Ba(Fe$_{0.925}$Co$_{0.075}$)$_2$As$_2$ single crystals

N. Haberkorn,[1,*] B. Maiorov,[1] I. O. Usov,[2] M. Weigand,[1] W. Hirata,[3] S. Miyasaka,[3] S. Tajima,[3] N. Chikumoto,[4] K. Tanabe,[4] and Leonardo Civale[1]

[1]*Los Alamos National Laboratory, Los Alamos, New Mexico 87545, USA*
[2]*MST-7, Los Alamos National Laboratory, Los Alamos, New Mexico 87545, USA*
[3]*Osaka University, 1-1 Machikaneyama, Toyonaka, Osaka 560-0043, Japan*
[4]*Superconductivity Research Laboratory-ISTEC, 1-10-13 Shinonome, Koto-ku, Tokyo 135-0062, Japan*

In this work we analyze the influence of random point defects introduced by 3 MeV proton irradiation on the critical current density (J_c) and vortex dynamics of a Ba(Fe$_{0.925}$Co$_{0.075}$)$_2$As$_2$ single crystal. The results show that at low temperatures (T) the irradiation produces an enhancement of J_c of up to 2.6 times. However the J_c (T) retention at different magnetic fields (H) in the elastic regime, estimated by the n exponent in J_c vs $(1 - (T/T_c)^2)^n$, is poorer after the irradiations due to the thermal softening of the pinning by the random point defects. We found that the elastic-to-plastic crossover and melting lines are only affected by the reduction of the superconducting critical temperature (T_c); they are exactly the same after rescaling the phase diagram by T/T_c. The pinning mechanisms in the single crystals can be associated with a mixed pinning landscape that produces a modulation in $S(H, T)$ as a consequence of a fishtail or second peak in the magnetization.

I. INTRODUCTION

Since the discovery of superconductivity in iron-based superconductors much effort has been devoted to understanding their properties.[1] Iron arsenide superconductors of the type AFe$_2$As$_2$ (122 system), where A is an alkaline-earth element, show intermediate superconducting transition temperatures (T_c) between that of conventional low T_c superconductors (LTS) and of cuprate high temperature superconductors (HTS), low anisotropy (γ), and high upper critical fields (H_{c2}), which are a consequence of the small coherence length (ξ). The fast dynamics (large creep rate S) in cuprates is due to the small pinning energy scale $(H_c^2/8\pi)(\xi^3/\gamma)$, which allows for a large influence of thermal fluctuations.[2] The study of vortex matter in 122 compounds provides an excellent opportunity to understand the crossover between LTS and HTS behavior.

For instance, recently we reported a glassy relaxation in optimally Na-doped CaFe$_2$As$_2$ single crystals ($T_c \sim 33$ K) with glassy exponent μ consistent with the predictions of the collective creep theory previously applied to cuprate superconductors.[3] On the other hand, in the underdoped system ($T_c \sim 19$ K) a glassy dynamics was also observed but with a μ larger than the collective creep models' predictions. An appealing aspect of those Na-doped CaFe$_2$As$_2$ crystals was their very simple pinning landscape, consisting almost exclusively of randomly distributed nanoparticles, which drastically simplifies the analysis.

Among the pnictide superconductors one of the most studied compounds is Co-doped BaFe$_2$As$_2$,[4] where high flux creep rates and a transition from collective to plastic creep have been reported.[5–7] This transition is similar to what was previously found in YBa$_2$Cu$_3$O$_7$ single crystals,[8] and we have also observed in it the Na$_x$Ca$_{1-x}$Fe$_2$As$_2$ single crystals. The pinning landscape in Co-doped BaFe$_2$As$_2$ is more complex, and different sources of pinning have been discussed, such as twin boundaries (TBs)[9,10] and nanoscale variations of T_c and/or

the superfluid density due to an inhomogeneous distribution of dopant atoms that produce modulations of the pinning energy.[11] This mixed landscape produces a fishtail effect in the critical current density (J_c) and more complex dependences in $S(T, H)$.

One way to understand the pinning mechanisms and the vortex dynamics in superconductors is by the artificial introduction of additional defects. Although random defects can be produced by chemical doping[12] and large defects by precipitation of secondary phases,[13] radiation damage is perhaps the most powerful procedure to controllably introduce defects into a material.[14–20] Recently, Nakajima *et al.*[18] showed that is possible to improve J_c in Co-doped material by the introduction of columnar defects (CD). Irradiation with gold produces discontinuous CD with diameters of 2–5 nm.[21] Also their results suggest that the crossover temperature from elastic to plastic (fast creep) increases after the irradiation,[18] which is consistent with a non-negligible influence of the ξ-to-defect size ratio and the presence of strong pinning centers.[3] An important remaining question is whether point defects are effective pinning centers in 122 superconductors having intermediate ξ between those of LTS and HTS.

In this work we analyze the influence of random point defects introduced by 3 MeV proton irradiation in a Ba(Fe$_{0.925}$Co$_{0.075}$)$_2$As$_2$ single crystal. The 3 MeV protons are known to create from one to a few tens of atom displacements,[14] producing mainly random point defects and also some nanoclusters of a few nanometers in size. At low temperatures (T) the irradiation produces an enhancement of J_c by a factor of up to 2.6. Both thermal fluctuations and the increase in $\xi(T)$ produce a reduction of the pinning effectiveness of the point defects as T increases. We found that the location of the elastic-to-plastic crossover and the melting line are not affected by the irradiation after rescaling the phase diagram by T/T_c.
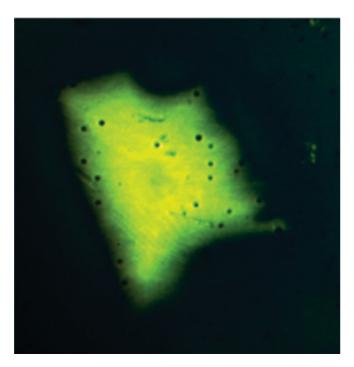
FIG. 1. (Color online) Magneto-optical image of $Ba(Fe_{0.925}Co_{0.075})_2As_2$ single crystal at $T = 3.88$ K in the remanent state after decreasing the magnetic field from 0.2 T.

II. EXPERIMENTAL

The single crystal [a rectangular plate of dimensions 1.2 (length, l) × 0.8 (width, w) × 0.03 (thickness, t) mm^3, with c axis parallel to t] was grown by the FeAs/CoAs self-flux method.[22] The Co content of the crystal was analyzed by using a field-emission electron probe micro analyzer (FE-EPMA) at 5–10 different points and confirmed to be uniform at $x = 0.075$, while the nominal composition was $x = 0.10$. We also confirmed by magneto-optical observation that the sample consisted of a single domain and was not granular (see Fig. 1). It was irradiated twice with 3 MeV protons to cumulative doses of 1×10^{16} cm^{-2} (F1) and 2×10^{16} cm^{-2} (F2). The magnetization (**M**) measurements were performed using a superconducting quantum interference device (SQUID) magnetometer for two applied magnetic field (**H**) configurations: **H** parallel to the c axis (**H** $\parallel$ c) and **H** rotated (along an axis parallel to l) by an angle $\Theta = 45°$ from the c axis (**H**$\parallel$45°). The J_c values were calculated from the magnetization data using the appropriate geometrical factor in the Bean Model.[23] For **H** $\parallel$ c, $J_c = \frac{20\Delta M}{w(1-w/3l)}$, where ΔM is the difference in magnetization between the top and bottom branches of the hysteresis loop. For **H**$\parallel$45°, both the longitudinal (M_l, parallel to **H**) and transverse (M_t, perpendicular to **H**) components

of **M** were measured, and J_c was calculated as described in further discussion. The creep measurement [$M(t)$] was recorded over a time of 1 hour. The initial time was adjusted considering the best correlation factor in the log-log fitting of the $M(t)$ dependence. The initial critical state for each creep measurement was generated using $\Delta H \sim 4\,H^*$, where H^* is the field for full-flux penetration.[24]

III. RESULTS

Irradiation with 3 MeV protons produces mostly Frenkel pairs, i.e., random point defects. Table I shows the cumulative amount of displacement damage (displacements per atom, dpa) after each dose, as estimated using the SRIM code,[25] as well as the average distance between defects. Also shown in Table I are the T_c values, determined from $M(T)$ at $H = 1.5$ Oe applied after zero field cooling, which are 24.4 K in the as-grown (AG) condition, 23.7 K after F1, and 22.4 K after F2. The change in T_c is consistent with previously reported data and the presence of nonmagnetic scattering centers.[26] The single crystal shows perfect diamagnetism, indicating full superconducting volume.

Figure 2 shows $J_c(H)$ at four different temperatures ($T = 5, 10, 15,$ and 20 K). The J_c (5 K, $H = 0$) increases from 0.75 MA cm^{-2} to 1.78 MA cm^{-2} and 1.83 MA cm^{-2}, for AG, F1, and F2, respectively. In the AG single crystal, $J_c(H)$ is characterized by the presence of a fishtail or second peak in the magnetization in the entire temperature range analyzed.[5] In F1 and F2 the fishtail disappears, masked by the additional pinning introduced by the irradiation. However, at high T (15 K and 20 K in Fig. 2) a hint of it is still visible as a reduction of the rate of decrease of J_c with H in the field range where J_c was increasing with H in the AG state. Also, at these high temperatures the fast drop in $J_c(H)$ begins at a lower H in the irradiated crystal. As we will discuss later, however, this is only a T_c reduction effect; the crossover to fast or plastic creep[5,7] and the location of the melting line (B_m) are not affected by the irradiations when the temperature is normalized by T_c.

To discriminate random and correlated pinning contributions, in Fig. 3 we show a comparison between the J_c vs H in AG [Fig. 3(a)] and F1 [Fig. 3(b)] for **H**$\parallel$$c$ and **H**$\parallel$45°. The analysis of magnetization loops for $\Theta \neq 0$ is more involved than for $\Theta = 0$ (**H**$\parallel$$c$). First we determined the longitudinal and transverse components of the irreversible magnetization ΔM_l and ΔM_t, and we experimentally confirmed that Δ**M** was normal to the crystal surface within the experimental error, as expected and previously observed[27] for a plate-like geometry as long as Θ is not too close to 90°. Then we calculated the irreversible magnetization $\Delta M = (\Delta M_l^2 + \Delta M_t^2)^{1/2}$. The main complication to obtain J_c from ΔM is that, in general, for

TABLE I. Summary of proton irradiation dose, displacements per atom (dpa), average distance between defects, and the resulting superconducting critical temperature (T_c) and critical current density (J_c) at $H = 0$ and 5 K.

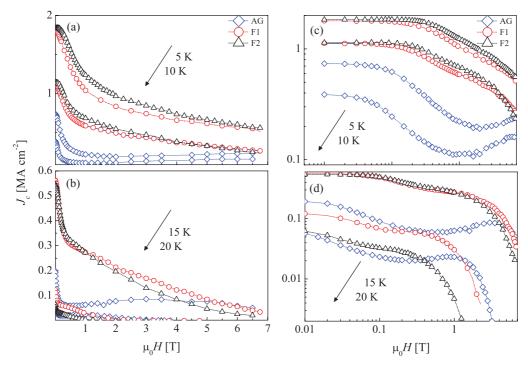| SC	3 MeV proton dose [cm^{-2}]	dpa	Defect distance [nm]	T_c [K]	J_c [H = 0, 5 K] MA cm^{-2}
AG	–	0	–	24.4	0.75
F1	1×10^{16}	8.7×10^{-4}	3.6	23.7	1.78
F2	2×10^{16}	1.7×10^{-3}	2.8	22.4	1.83

FIG. 2. (Color online) Critical current density (J_c) vs magnetic field (H) at 5, 10, 15, and 20 K in the AG single crystal (open rhombus) and after the two proton irradiations: F1 (open circles) and F2 (open triangles). The same data is shown in linear [panels (a) and (b)] and log-log [panels (c) and (d)] scales.

$\Theta \neq 0$ the orientation of the vortices (i.e., the angle Θ_B between the internal field **B** and the c axis) is not parallel to **H**,[28,29] so the critical state relates to $J_c(\Theta_B)$ rather than to $J_c(\Theta)$. Moreover, although for any Θ_B the current flowing parallel to l (the long pair of sides of the rectangular crystal) is perpendicular to the vortices (maximum Lorentz force configuration); the current parallel to w (the short sides) is not, so the effective J_c in those sides is approximately $J_c/\cos(\Theta_B)$, and using the anisotropic version of the critical state Bean model (see sketch in Fig. 5 of Ref. 30), we obtain

$$J_c(\Theta_B) = \frac{20\Delta M}{w(1 - w\cos(\Theta_B)/3l)}. \tag{1}$$

Both the sign and magnitude of the misalignment Θ_B-Θ depend on γ and the geometry of the sample (demagnetizing factors).[29] In all cases Θ_B-Θ vanishes approximately as $1/H$ at high fields (the free energy minimizes for **B**∥**H**), while for the particular parameters of our crystal (which is in the "geometry dominated case" in the classification of Ref. 26) in the low H limit $\Theta_B \to 0$ (the system minimizes the free energy by reducing the length of the vortices). In Fig. 3 we plot two $J_c(H)$ curves for each dataset at **H**∥45°. The green triangles are obtained from Eq. (1) with $\Theta_B = 0$, as expected at low H, while the blue circles are calculated from Eq. (1) with $\Theta_B = \Theta$, the situation expected at high H. In this last case we only show data where $|\Theta_B$-$\Theta| < 1°$ for the particular conditions of our measurements.
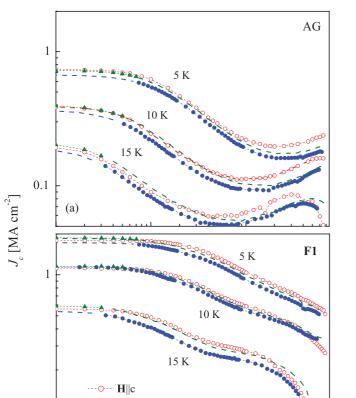
In a single-band anisotropic superconductor,[2] the anisotropic scaling approach predicts that if pinning is only due to random point defects, then $J_c(H, \Theta)$ depends only on the rescaled field $\varepsilon(\Theta, \gamma)H$, where $\varepsilon(\Theta, \gamma) = [\cos^2\Theta + \gamma^{-2}\sin^2\Theta]^{1/2}$. For instance, in YBCO thin films
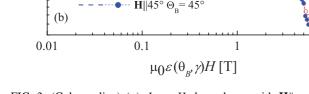
with small amounts of correlated disorder, J_c follows this scaling rule over large portions of the (T-H-Θ) space.[31] It is thus useful to compare the field dependence of J_c at different orientations as a function of $\varepsilon(\Theta, \gamma)H$, so if pinning is only due to random point defects the curves will overlap, and the absence of overlap indicates the presence of other pinning mechanisms. It is important to recognize that this analysis is consistent only if the γ used in the J_c scaling is the same as obtained by direct measures of the mass anisotropy, e.g., from the angular dependence of the upper critical field H_{c2}. In the iron-based superconductors the anisotropic temperature dependence of the gap results in a temperature dependence of γ that must be taken into account. Recently, Kidszun *et al.*[32] have shown that the anisotropic scaling approach can be successfully applied to describe $J_c(H, \Theta)$ in LaFeAsO$_{1-x}$F$_x$ thin films with a temperature-dependent γ.

The anisotropic scaling rule is valid at high fields where the misalignment between **B** and **H** described previously can be disregarded. In Fig. 3 the horizontal axis is $\varepsilon(\Theta_B, \gamma)H$, where we used $\Theta_B = \Theta = 45°$ for the blue circle curves (as dictated by the anisotropic scaling rule) but chose $\Theta_B = 0$ for the green triangle curves to account for the fact that vortices are pointing close to the c axis. We also used a temperature-dependent γ. The values of γ for each temperature (the same for the blue circles and green triangles) were taken from Ref. 33, being 1.2, 1.5, and 2 for 5 K, 10 K, and 15 K, respectively, i.e., they are not adjustable parameters.

The first observation from Figs. 3(a) and (b) is that the difference between the two limits used to describe the **H**∥45° data ($\Theta_B = 45°$ and $\Theta_B = 0$) is not large. At intermediate fields a smooth crossover between both curves should occur as Θ_B evolves from 0 to 45°. Second, at low H the **H**∥c

FIG. 3. (Color online) (*a*) J_c vs *H* dependence with **H**∥*c* and **H**∥45° in the as-grown (AG) crystal. (*b*) J_c vs *H* dependence with **H**∥*c* and **H**∥45° after the first irradiation (F1). For **H**∥45° two estimates for $J_c(H)$ according to Eq. (1) are included, with $\Theta_B = 0$ (**B**∥*c* axis) for low fields and $\Theta_B = 0$ (**B**∥**H**) for high fields.

and $\Theta_B = 0$ data coincide both for AG and F1, as expected. For AG [Fig. 3(a)], J_c at the fishtail is higher in the **H**∥*c* than in the **H**∥45° configuration, which indicates that the pinning can be associated with correlated disorder. In Refs. 5 and 9 the fishtail for the same compound was attributed to the presence of domain walls propagating along the *c* axis. However, this feature is also observed in over-doped Ba(Fe$_{1-x}$Co$_x$)$_2$As$_2$ with $x = 0.08$–0.15 where the domain wall is absent (Ref. 7), indicating that a fishtail may also originate from other correlated pinning mechanisms. At intermediate magnetic fields, where $J_c(H)$ approximately follows a power-law dependence $J_c \propto H^{-\alpha}$, the coincidence of the exponent α for **H**∥*c* and **H**∥45° suggests that the pinning is dominated by the same kind of disorder in both configurations. The same comparison between **H**∥*c* and **H**∥45° in F1 [Fig. 3(b)] shows that the irradiation introduces mainly random disorder, which is in agreement with expectations. The slightly higher J_c for **H**∥*c* than for **H**∥45° in this case indicates that the correlated pinning originally present in AG is still active.

The modulation of the creep rate ($S = -\frac{\delta(\ln J_c)}{\delta(\ln t)}$) along the fishtail has been previously discussed.[5,18,34] As shown in Fig. 3,
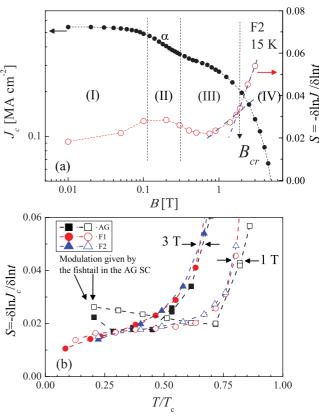

FIG. 4. (Color online) (a) Magnetic field (*B*) dependence of J_c and the creep rate ($S = -\frac{\delta(\ln J_c)}{\delta(\ln t)}$) in F2 at 15 K. (b) Creep rate (*S*) vs reduced temperature (T/T_c) with $B = 1$ T and $B = 3$ T for the single crystal AG, and after of F1 and F2.

the random point defects created by the irradiations mask this feature in our crystal, however, the associated modulation of the $S(H)$ dependence at high temperatures remains visible after the irradiations. Figure 4(a) shows the magnetic field dependence of J_c and S in F2 at 15 K. $J_c(H)$ shows different regimes: (I) A low-field regime ($B < B^*$) that could be associated with
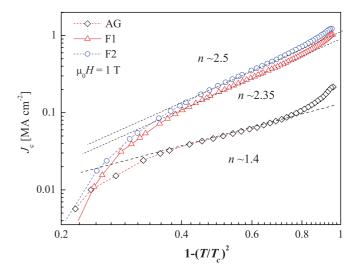

FIG. 5. (Color online) J_c vs. $(1 - (\frac{T}{T_c})^2)$ dependence at 1 T in AG, F1, and F2; the straight lines correspond to the best fits to obtain the *n* value.
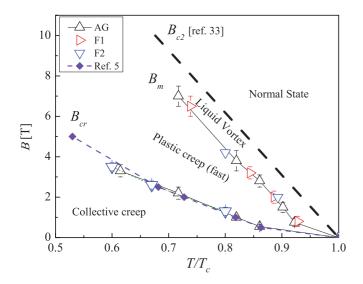
FIG. 6. (Color online) Vortex phase diagram B-T/T_c in the AG and irradiated single crystal. The B_{c2} line was obtained from Ref. 33. For comparison to other results on similar materials the elastic to plastic crossover (B_{cr}) from Ref. 5 was included.

the single vortex regime[35] but that is also strongly affected by self-field effects;[3,36–38] (II) a power-law dependence $J_c \propto H^{-\alpha}$, which can be associated with strong pinning centers;[35,39] (III) a third regime associated with the fishtail in the AG state, where $J_c(H)$ decreases more slowly with H and $S(H)$ shows a minimum; and (IV) a high-field regime where the vortex dynamics are plastic instead of elastic, which is characterized by a fast drop in $J_c(H)$ and a fast increase in $S(H)$.[5,7] The crossover line between elastic and plastic dynamics (the boundary between regimes III and IV) is the crossover field $B_{cr}(T)$, to be discussed further (Fig. 6). The upper end of regime IV is the melting line $B_m(T)$, also shown in Fig. 6, which we estimated from the disappearance of hysteresis in isothermal magnetization loops within our experimental resolution ($J_c \sim 100$ A/cm^2). The $S(H)$ data equivalent to that in Fig. 4(a) for the AG crystal is similar to what has previously been reported. Briefly, $S(H)$ shows a maximum around the lower end of the fishtail [the minimum in $J_c(H)$], then decreases as $J_c(H)$ increases, and finally starts to increase rapidly around the maximum in $J_c(H)$, indicating the elastic-to-plastic crossover in the vortex dynamics.[5,7,18] Figure 4(b) shows S for AG, F1, and F2 at $H = 1$ T and 3 T as a function of reduced temperature T/T_c. It is apparent that the data for F1 and F2 are almost identical. The AG crystal shows higher S at low T, associated with the previously mentioned maximum in S related to the fishtail. However at high T, in the elastic-to-plastic crossover region, the $S(T/T_c)$ data is also similar to the that of the irradiated states.

IV. DISCUSSION

The results indicate that J_c in Co-122 single crystals can be enhanced by random point defects created by irradiation with protons, and the data in Fig. 3 confirms that the introduced pinning is random. Additional information about pinning mechanisms can be obtained from $J_c(T)$, which is predicted to follow the dependence $J_c \propto (1 - (\frac{T}{T_c})^2)^n$.[40] In the limit of

single vortex pinning, the exponent n is ~ 1.2 and ~ 2.5 for pinning arising from variations in T_c and in the electronic mean free path (δT_c and δl pinning), respectively.[2] The first case corresponds to strong pinning by extended defects, such as random nanoparticles, while the second one applies to point defects. This dependence has been confirmed, for instance, in YBCO thin films where pinning is dominated by random nanoparticles with $n \sim 1.25$ to 1.35, in good agreement with expectation.[41] We have recently observed the same behavior in Na$_x$Ca$_{1-x}$Fe$_2$As$_2$ single crystals, with $n \sim 1.2$ and ~ 1.4 in the nanoparticle-dominated pinning regime for $x = 0.5$ and $x = 0.75$, respectively.[3]

Figure 5 shows J_c vs $1 - (T/T_c)^2$ for AG, F1, and F2 at $\mu_0 H = 1$ T for $\mathbf{H} \| c$. Although this field does not strictly correspond to the single vortex limit, our Na$_x$Ca$_{1-x}$Fe$_2$As$_2$ single crystal studies showed that the n values are essentially magnetic field independent. We observe that in AG $n \sim 1.4$, consistent with δT_c pinning associated with the naturally grown extended defects, increasing to $n \sim 2.35$ for F1 and $n \sim 2.5$ for F2, indicating a transition to point-defect-dominated pinning.

The ratio of the vortex core size at a given temperature [$\sim \xi(T)$] to the defects size is a key parameter in determining pinning strength. It is well known that defects much smaller than $\xi(T)$ are not effective as pinning centers. Point defects are effective in oxide HTS at $T \ll T_c$ because of their very small coherence length [e.g., in YBCO $\xi(0) \approx 1.2$ nm],[2] and irradiation studies in conventional LTS have shown[42] that point defects do not increase J_c in materials with much larger $\xi(0)$. In our optimally Co-doped 122 single crystal, $\xi(0) \approx 2.58$ nm,[33] and our results demonstrate that point defects are still effective pinning centers in this case.

The dpa estimates (Table I) imply densities of point defects of $\sim 2.2 \times 10^{19}$ cm^{-3} and $\sim 4.4 \times 10^{19}$ cm^{-3} (average distance between defects 3.6 nm and 2.8 nm) for F1 and F2, respectively. These densities must be taken as upper limits due to two factors. First, some of the primary point defects may migrate to form small clusters, and second, some defects may anneal out. Although the first effect is probably very small, the second one is likely to be significant. Studies in YBCO crystals have shown that the optimum J_c for proton irradiations was obtained for average distances between point defects of the order of ξ. We have chosen our doses to achieve a similar situation in our Co-doped 122 single crystal, thus the obtained J_c values are probably close to the upper limit of what can be attained by point defects. Two observations additionally support this idea, namely the almost identical J_c values in F1 and F2, indicating saturation, and the large decrease in T_c (fractionally much larger than in YBCO irradiated to the optimum dose), suggesting that further irradiations would drastically degrade the superconducting properties.

Considering $\lambda(0) = 260$ nm[43] and $\xi(0) = 2.58$ nm,[33] we can estimate the thermodynamic critical field $H_c(T = 0K) = \Phi_0/(2\sqrt{2}\pi\lambda\xi) \approx 0.34T$ and the depairing current density $J_0(T = 0K) = cH_c/3\sqrt{6}\pi\lambda \approx 57$ MAcm^{-2}, thus at 5 K and low fields, $(J_c/J_0) \approx 0.013$ in AG and $(J_c/J_0) \approx 0.03$ in F1 and F2. For comparison, the highest J_cs reported for proton-irradiated YBCO (at low T and H) are ~ 20 MA/cm^2, or $\sim 0.07 J_0$. This roughly $2\times$ difference is easily understood by considering that the effectiveness of point defects decreases with ξ. On the other hand, Nakajima *et al.*[18] showed that in

Co-doped $BaFe_2As_2$ single crystals, the introduction of defects by heavy ion irradiation produces $J_c \sim 4$ MA cm^{-2} (at 5 K and $H = 0$), i.e., $(J_c/J_0) \approx 0.07$.

The effects of the irradiation are more important at low temperatures, as is clearly seen in Fig. 5, which shows that as T approaches T_c, the J_c in F1 and F2 becomes similar to AG, even when plotted vs reduced temperature. This is consistent with weak pinning by random point defects[2] and is due to two factors: the increase in $\xi(T)$ and the reduction of pinning by thermal fluctuations. Considering a highly localized core-pinning mechanism on the scale of the coherence length, when the mean-square thermal displacement of the vortices exceeds the core radius ($\langle u^2 \rangle^{1/2} > \sqrt{2}\xi$) the strength of the pinning will be strongly reduced.[2,44]

The H-T/T_c vortex phase diagram presented in Fig. 6 shows that indeed neither $B_{cr}(T)$ nor $B_m(T)$ are affected by the successive irradiations. Following the procedure used previously,[5] in the AG crystal $B_{cr}(T)$ is defined as the field at the maximum J_c in the fishtail, which coincides with the fast increase in $S(H)$. In the irradiated samples $B_{cr}(T)$ is defined by the field where the creep starts to be fast with a resulting drop in the $J_c(H)$ dependence [see Fig. 4(a)]. Clearly the elastic-to-plastic crossover[5,7] is not affected by the proton irradiation when plotted vs T/T_c, which indicates that the pinning centers that dominate at high temperature are the same in the AG, F1, and F2, namely the naturally grown extended defects. In contrast, inspection of Fig. 4(b) in Ref. 18 suggests that the larger defects created by heavy ion irradiation in Co-doped $BaFe_2As_2$ single crystals are dominant and the ones effective at increasing B_{cr} at 15 K.

Finally, Fig. 6 shows the irreversibility or melting line $B_m(T)$, which again is unchanged by the irradiation. It is worth mentioning that early studies in YBCO single crystals had also shown that $B_m(T)$ was not altered by proton irradiation. The presence of a vortex liquid in 122 pnictides was previously discussed.[36,45,46] As we have done for $Na_xCa_{1-x}Fe_2As_2$ single crystals, we can use the Lindeman criterion as a simple way to estimate the vortex lattice melting line, $B_m(T) \approx (5.6c_L^4/G_i)H_{c2}(1 - T/T_c)^2$,[2] where $Gi = \frac{1}{2}[\frac{\gamma T_c}{H_c^2(0)\xi^3(0)}]^2$ is the Ginzburg number, the parameter governing the strength of the thermal fluctuations. The temperature-dependent γ introduces an uncertainty in Gi; if we consider the whole range $\gamma = 1.2$ to 3.5[33] for this compound, then $Gi = 0.0002$–0.0016. Even larger is the uncertainty associated with the Lindeman parameter: $c_L \approx 0.1$–0.4. If we consider $c_L \sim 0.1$–0.14, we find that a narrow vortex-liquid phase is possible, consistent with our data.

In the glassy regime below $B_{cr}(T)$ in the phase diagram (Fig. 6), $S = \frac{T}{U_0 + \mu T \ln(t/t_0)}$, where the glassy exponent μ is regime-dependent.[2] Above a characteristic temperature this simplifies to $S = [\mu \ln(t/t_0)]^{-1}$. In the simplest collective creep descriptions μ should be constant for a given regime, thus $S(H, T)$ should be independent of *both* T and H in that region of the phase diagram. This is exactly what we previously observed in $Ca_{1-x}NaxFe_2As_2$ single crystals,[3,36] because in that case the pinning landscape was particularly simple, essentially consisting only of randomly distributed nanoparticles. In the present case, in contrast, $S(T, H)$ below $B_{cr}(T)$ is affected by the presence of the fishtail and shows significant modulations (in the range $0.01 < S < 0.04$), which do not allow the identification of a plateau in $S(T, H)$. The reason for this behavior is that the pinning in Co-doped $BaFe_2As_2$ results from a combination of defects that may include nanoprecipitates,[35,36] TBs,[9,10] local inhomogeneities,[11] and in the case of the proton irradiated samples, also high density of random point defects. These variations in $S(T, H)$ for $B < B_{cr}$, as well as the boundaries of the $J_c \propto H^{-\alpha}$ regime were not included in the phase diagram because they are strongly affected by annealing.[47]

V. CONCLUSION

We have studied the influence of random point defects introduced by proton irradiation into Co-doped $BaFe_2As_2$ single crystals. Our results show that at low temperatures (5 K, $H = 0$) the J_c values in the irradiated single crystal (F1 and F2) can be increased in a factor up to 2.6 (0.03 J_0) in comparison with the AG single crystal (~ 0.013 J_0). Both fluctuations and the $\xi(T)$ increase are important in the reduced effectiveness (thermal softening) of the pinning by random defects as T increases. The J_c (T) retention is poorer in the irradiated samples, and T_c decreases systematically as a consequence of structural damage. We found that the elastic-to-plastic crossover and B_m line are only affected by the reduction of T_c but are exactly the same after rescaling the phase diagram by T/T_c. We do not observe a plateau in $S(T)$ associated with glassy relaxation, which could be due to the modulation in $J_c(H)$ given the presence of a fishtail, or second peak, in the magnetization that remains after irradiation. A narrow liquid phase region was identified, which is consistent with the expectation of the Lindeman criterion.

---

*nhaberkorn@lanl.gov

[1]J. Paglione and R. L. Greene, Nature Physics **6**, 645 (2010).

[2]G. Blatter, M. V. Feigel'man, V. B. Geshkenbein, A. I. Larkin, and V. M. Vinokur, Rev. Mod. Phys. **66**, 1125 (1994).

[3]N. Haberkorn, M. Miura, B. Maiorov, G. F. Chen, W. Yu, and L. Civale, Phys. Rev. B **84**, 094522 (2011).

[4]A. S. Sefat, R. Jin, M. A. McGuire, B. C. Sales, D. J. Singh, and D. Mandrus, Phys. Rev. Lett. **101**, 117004 (2008).

[5]R. Prozorov, N. Ni, M. A. Tanatar, V. G. Kogan, R. T. Gordon, C. Martin, E. C. Blomberg, P. Prommapan, J. Q. Yan, S. L. Bud'ko, and P. C. Canfield, Phys. Rev. B **78**, 224506 (2008).

[6]A. Yamamoto, J. Jaroszynski, C. Tarantini, L. Balicas, J. Jiang, A. Gurevich, D. C. Larbalestier, R. Jin, A. S. Sefat, M. A. McGuire, B. C. Sales, D. K. Christen, and D. Mandrus, Appl. Phys. Lett. **94**, 062511 (2009).

[7]B. Shen, P. Cheng, Z. Wang, L. Fang, C. Ren, L. Shan, and H. H. Wen, Phys. Rev. B **81**, 014503 (2010).

[8]Y. Abulafia, A. Shaulov, Y. Wolfus, R. Prozorov, L. Burlachkov, Y. Yeshurun, D. Majer, E. Zeldov, H. Wühl, V. B. Geshkenbein, and V. M. Vinokur, Phys. Rev. Lett. **77**, 1596 (1996).

[9]R. Prozorov, M. A. Tanatar, N. Ni, A. Kreyssig, S. Nandi, S. L. Bud'ko, A. I. Goldman, and P. C. Canfield, Phys. Rev. B **80**, 174517 (2009).

[10]B. Kalisky, J. R. Kirtley, J. G. Analytis, J.-H. Chu, I. R. Fisher, and K. A. Moler, Phys. Rev. B **83**, 064511 (2011).

[11]S. Demirdis, C. J. vanderBeek, Y. Fasano, N. R. CejasBolecek, H. Pastoriza, D. Colson, and F. Rullier-Albenque, Phys. Rev B **84**, 094517 (2011).

[12]L. M. Paulius, C. C. Almasan, and M. B. Maple, Phys. Rev. B **47**, 11627 (1993).

[13]M. Murakami, H. Fujimoto, S. Gotoh, K. Yamaguchi, N. Koshizuka, and S. Tanaka, Physica C **185–189**, 321 (1991).

[14]L. Civale, A. D. Marwick, M. W. McElfresh, T. K. Worthington, A. P. Malozemoff, F. H. Holtzberg, J. R. Thompson, and M. A. Kirk, Phys. Rev. Lett. **65**, 1164 (1990).

[15]L. Civale, A. D. Marwick, T. K. Worthington, M. A. Kirk, J. R. Thompson, L. Krusin-Elbaum, Y. Sun, J. R. Clem, and F. Holtzberg, Phys. Rev. Lett. **67**, 648 (1991).

[16]M. Konczykowski, F. Rullier-Albenque, E. R. Yacoby, A. Shaulov, Y. Yeshurun, and P. Lejay, Phys. Rev. B **44**, 7167 (1991).

[17]R. Prozorov, M. A. Tanatar, B. Roy, N. Ni, S. L. Bud'ko, P. C. Canfield, J. Hua, U. Welp, and W. K. Kwok, Phys. Rev. B **81**, 094509 (2010).

[18]Y. Nakajima, Y. Tsuchiya, T. Taen, T. Tamegai, S. Okayasu, and M. Sasase, Phys. Rev. B **80**, 012510 (2009).

[19]T. Taen, Y. Nakajima, T. Tamegai, H. Kitamura, and T. Murakami, Physica C **471**, 784 (2011).

[20]L. Fang, Y. Jia, J. A. Schlueter, A. Kayani, Z. L. Xiao, H. Claus, U. Welp, A. E. Koshelev, G. W. Crabtree, and W.-K. Kwok, Phys. Rev. B **84**, 140504 (2011).

[21]T. Tamegai, Y. Tsuchiya, T. Taen, Y. Nakajima, S. Okayasu, and M. Sasase, Physica C **470**, S360 (2010).

[22]N. Ni, M. E. Tillman, J.-Q. Yan, A. Kracher, S. T. Hannahs, S. L. Bud'ko, and P. C. Canfield, Phys. Rev. B **78**, 214515 (2008).

[23]C. P. Bean, Phys. Rev. Lett. **8**, 250 (1962); Rev. Mod. Phys. **36**, 31 (1964).

[24]Y. Yeshurun, A. P. Malozemoff, and A. Shaulov, Rev. Mod. Phys. **68**, 911 (1996).

[25]J. F. Ziegler, J. P. Biersack, and U. Littmark, *The Stopping and Range of Ions in Solids* (Pergamon, New York, 1985).

[26]Y. Nakajima, T. Taen, Y. Tsuchiya, T. Tamegai, H. Kitamura, and T. Murakami, Phys. Rev. B **82**, 220504 (R) (2010).

[27]F. Hellman, E. M. Gyorgy, and R. C. Dynes, Phys. Rev. Lett. **68**, 867 (1992); L. Klein, E. R. Yacoby, Y. Wolfus, Y. Yeshurun,

L. Burlachkov, B. Y. Shapiro, M. Konczykowski, and F. Holtzberg, Phys. Rev. B **47**, 12349 (1993).

[28]V. G. Kogan, Phys. Rev. B **38**, 7049 (1988).

[29]A. V. Silhanek, L. Civale, and M. A. Avila, Phys. Rev. B **65**, 174525 (2002).

[30]J. R. Thompson, J. W. Sinclair, D. K. Christen, Y. Zhang, Y. L. Zuev, C. Cantoni, Y. Chen, and V. Selvamanickam, Supercond. Sci. Technol. **23**, 014002 (2010).

[31]L. Civale, B. Maiorov, A. Serquis, J. O. Willis, J. Y. Coulter, H. Wang, Q. X. Jia, P. N. Arendt, M. Jaime, J. L. MacManus-Driscoll, M. P. Maley, and S. R. Foltyn, J. Low Temp. Phys. **135**, 87 (2004).

[32]M. Kidszun, S. Haindl, T. Thersleff, J. Hanisch, A. Kauffmann, K. Iida, J. Freudenberger, L. Schultz, and B. Holzapfel, Phys. Rev. Lett. **106**, 137001 (2011).

[33]M. Kano, Y. Kohama, D. Graf, F. Balakirev, A. S. Sefat, M. A. McGuire, B. C. Sales, D. Mandrus, and S. W. Tozer, J. Phys. Soc. Japan **78**, 084719 (2009).

[34]S. Salem-Sugui, L. Ghivelder, A. D. Alvarenga, L. F. Cohen, K. A. Yates, K. Morrison, J. L. Pimentel, H. Luo, Z. Wang, and H. H. Wen, Phys. Rev B **82**, 054513 (2010).

[35]J. van der Beek, G. Rizza, M. Konczykowski, P. Fertey, I. Monnet, Thierry Klein, R. Okazaki, M. Ishikado, H. Kito, A. Iyo, H. Eisaki, S. Shamoto, M. E. Tillman, S. L. Bud'ko, P. C. Canfield, T. Shibauchi, and Y. Matsuda, Phys. Rev B **81**, 174517 (2010).

[36]N. Haberkorn, B. Maiorov, M. Jaime, I. Usov, M. Miura, G. F. Chen, W. Yu, and L. Civale, Phys. Rev. B **84**, 064533 (2011).

[37]V. K. Vlasko-Vlasov, U. Welp, G. W. Crabtree, D. Gunter, V. Kabanov, and V. I. Nikitenko, Phys. Rev. B **56**, 5622 (1997).

[38]T. Taen, Y. Tsuchiya, Y. Nakajima, and T. Tamegai, Physica C **470**, 1106 (2010).

[39]C. J. van der Beek, M. Konczykowski, A. Abal'oshev, I. Abal'osheva, P. Gierlowski, S. J. Lewandowski, M. V. Indenbom, and S. Barbanera, Phys. Rev. B **66**, 024523 (2002).

[40]A. O. Ijaduola, J. R. Thompson, R. Feenstra, D. K. Christen, A. A. Gapud, and X. Song, Phys. Rev. B **73**, 134502 (2006).

[41]M. Miura, B. Maiorov, S. A. Baily, N. Haberkorn, J. O. Willis, K. Marken, T. Izumi, Y. Shiohara, and L. Civale, Phys. Rev. B **83**, 184519 (2011).

[42]H. C. Freyhardt, J. Low Temp. Phys. **32**, 101 (1978).

[43]L. Luan, T. M. Lippman, C. W. Hicks, J. A. Bert, O. M. Auslaender, J.-H. Chu, J. G. Analytis, I. R. Fisher, and K. A. Moler, Phys. Rev. Lett. **106**, 067001 (2011).

[44]L. Krusin-Elbaum, L. Civale, F. Holtzberg, A. P. Malozemoff, and C. Feild, Phys. Rev. Lett. **67**, 3156 (1991).

[45]H.-J. Kim, Y. Liu, Y. S. Oh, S. Khim, I. Kim, G. R. Stewart, and K. H. Kim, Phys. Rev. B **79**, 014514 (2009).

[46]B. Maiorov, T. Katase, S. A. Baily, H. Hiramatsu, T. G. Holesinger, H. Hosono, and L. Civale, Supercond. Sci. Technol. **24**, 055007 (2011).

[47]K. Gofryk, A. B. Vorontsov, I. Vekhter, A. S. Sefat, T. Imai, E. D. Bauer, J. D. Thompson, and F. Ronning, Phys. Rev. B **83**, 064513 (2011).